

TRACKING SIMULATIONS OF SHADOWING ELECTROSTATIC SEPTUM WIRES BY MEANS OF BENT CRYSTALS

F. M. Velotti*, M. A. Fraser, B. Goddard, V. Kain, L.S. Stoel,
CERN, Geneva, Switzerland

Abstract

The CERN Super Proton Synchrotron (SPS) slow extraction is a third integer resonant extraction and hence suffers from high losses at the electrostatic septum (ZS). This is one of the main limiting factors for the maximum number of Protons On Target (POT) deliverable from the SPS to the North Area (NA). A concept to significantly reduce the extraction losses via shadowing of the electrostatic septum wires using an upstream bent crystal has been proposed in [1], predicting a loss reduction of up to about 50% for the prototype system installed in 2018. Following the successful experimental demonstration of the concept with beam [2], detailed tracking simulations have been performed to fully understand the results obtained. Further insights, such as the effective ZS width and its alignment, could be deduced by exploiting the response of the extraction loss as a function of the two degrees of freedom of the crystal (position and angle). In this paper, the beam dynamics simulations are discussed together with the implementation of the bent crystal into the simulation framework. A comparison with measurements is presented before proposals for new configurations and parameters are discussed.

INTRODUCTION

The SPS hosts a slow extraction channel in the Long Straight Section (LSS) 2 which provides a constant flux of particles, in the order of seconds, to the experiments of the North Area (NA). By design, the resonant slow extraction is a lossy process as the electrostatic septum (ES, or ZS for the SPS) wires are directly used to separate the circulating beam from the extracted one. Two proposed solutions [1] foresee the exploitation of a silicon bent crystal to shadow the ES, either locally in LSS2 or non-locally elsewhere in the ring. Following the conceptual design and expected performance presented in [1], a prototype crystal was installed in the SPS in LSS2, 4° in betatron phase advance upstream the ZS. Details of the measurements campaign is discussed in [2].

A more complete description of the recent results described in this paper can be found in [3].

SIMULATION METHODOLOGY

Comprehensive particle tracking simulations that include the non-linear beam dynamics of the slow extraction process in the synchrotron, the beam-crystal and beam-septum interaction were essential to define the required layout, to understand the experimental results and to optimise the performance reach of the concept.

* francesco.maria.velotti@cern.ch

Beam-Crystal Interaction

The beam-crystal interaction was modelled using an empirical approach and by incorporating the behaviour measured by the UA9 collaboration in dedicated beam tests [4] as a 2D probability density function (PDF) in *pycollimate* [1]. The measured scattering response was transformed into a set of discrete mono-dimensional histograms as a function of the difference in angle of the incoming beam with respect to the channelling angle of the crystal. The measured data was binned at 5 μ rad so interpolation was required to produce the 2D PDF. The simulated response using this approach is essentially indistinguishable from the measured data. It is this PDF, implemented in *pycollimate*, which is used to calculate the effect of the crystal, as a function of its position and orientation, on the incoming beam.

Simplified Beam Dynamics Simulations

A simulation model of the SPS during slow extraction was built with MAD-X [5]. The machine tune is set on-resonance for on-momentum particles, i.e. $3\nu_x = 80$ for $\Delta p/p_0 = 0$. The normalised chromaticities are set to their measured values ($\xi_x = -1$, $\xi_y = 0.58$), and the extraction bump in LSS2 is turned on. With the implementation of Constant Optics Slow Extraction (COSE) methodology [6], the simulations could be simplified and their speed increased as the optics is theoretically frozen for all extracted particles throughout the spill. It is then only necessary to simulate one instance of the spill, ensuring that the stop-band width in relative momentum space ($\Delta p/p_0 \approx \pm 10^{-4}$) either side of the resonant tune is sufficiently covered. Two techniques were explored:

- Slicing the SPS sequence for thin lens tracking with internal MAD-X routines,
- Creating the PTC [7] sequence using MAD-X and extracting maps of the relevant portions of the SPS sequence to a given order.

The first method is pure thin lens tracking through every element of the SPS sequence. When a crystal-type element is encountered the particle distribution is handed over to *pycollimate* to evaluate the beam-crystal interaction for a given crystal configuration (position and orientation). This methodology has the advantage of being very accurate, permits aperture restrictions to be rigorously checked and can include time-dependent effects, however it is also time consuming due to the length of the SPS sequence and the hand-over of the particle distribution between MAD-X and *pycollimate* at every interaction.

Content from this work may be used under the terms of the CC BY 3.0 licence (© 2019). Any distribution of this work must maintain attribution to the author(s), title of the work, publisher, and DOI

The second method, instead, employs polymorphic maps generated from PTC at a given order to transport the particle distribution from one point to another in the machine using an external, custom script. The MAD-X interface allows to chose the integration steps and method used to create the PTC sequence. In this case, accurate tracking can be performed whilst significantly reducing the computation time, which was essential for the parametric scans needed to assess the performance of crystal shadowing concept presented in this paper.

To evaluate the accuracy of the methodology based on tracking with PTC sector maps extracted from MAD-X, a comparison was performed with PTC tracking (element-by-element) at the 20th order. The figure of merit chosen to evaluate the accuracy was the normalised variation of the horizontal action $\Delta J_x / J_x$, where the action is calculated as:

$$J_x = \frac{\bar{X}^2 + \bar{X}'^2}{2} \quad (1)$$

with \bar{X} and \bar{X}' being the horizontal normalised phase space coordinates. The results of the comparison is shown in Fig. 1 where a benchmark is presented using the SPS lattice configured for slow extraction. Clear convergence is observed as the map order is increased. Due to the time needed for very high-order maps, 4th-order maps were chosen as good compromise between accuracy and computational time. In fact, the maximum error between pure thick tracking element-by-element using PTC and sector maps at 4th order, for the lattice configuration under analysis, is less than 0.6% in horizontal action.

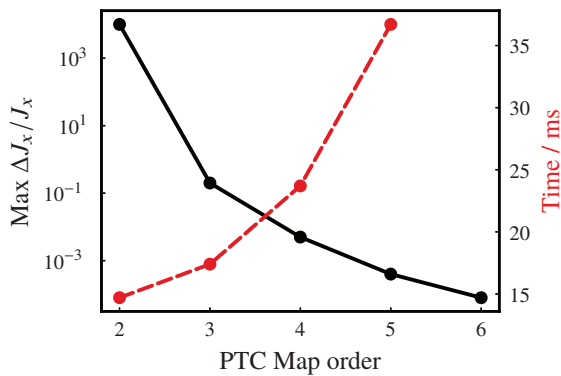
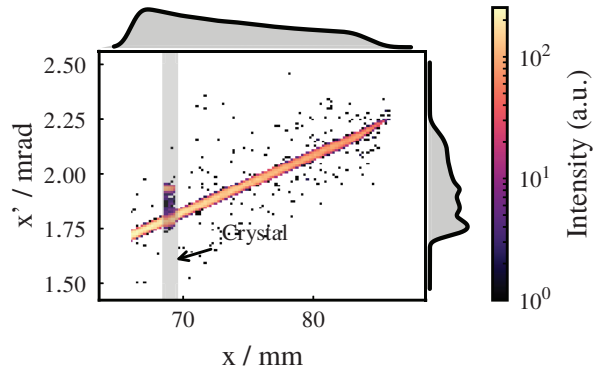


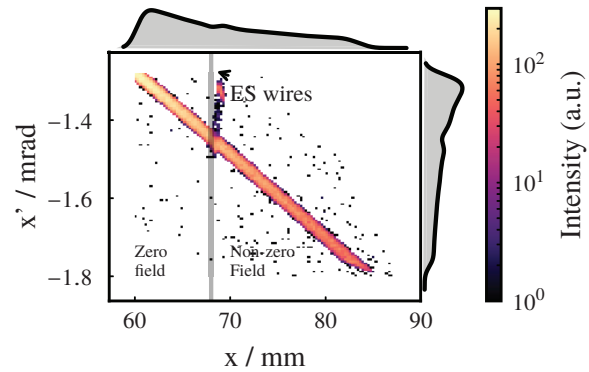
Figure 1: Comparison of tracking using sector maps extracted at different order from PTC and element-by-element tracking with MAD-X PTC at 20th-order.

LOCAL SHADOWING SIMULATIONS

A suitable location for the crystal in LSS2 was identified ~5 m upstream of the ES separated by a wide aperture focusing quadrupole and 4° of betatron phase advance. The small phase advance from the crystal to the ES is still adequate to demonstrate the shadowing concept. Using the simulation tools described in the previous section, tracking simulations were performed to specify the crystal characteristics needed



(a) At the crystal location.



(b) At the electrostatic septum location.

Figure 2: Shadowing of ES with a thin crystal. The trace space distribution (a) at the crystal of width 0.8 mm (shaded) is shown along with the coherently channelled particles, together with the trace space distribution (b) at the extraction septum. The channelled particles missing the thin wire-array (shaded) are clearly shown on the high-field side of the septum, transported into the extraction line.

to achieve loss reduction at the ES. In the simulation studies presented in this paper an effective ES thickness of 500 μm was assumed based on the results of empirical linear scans of the passive (wire-array) diffuser installed and tested with beam earlier in 2018 [8]. The parameters of the crystal used for the SPS tests were specified in [9] with a thickness of ~0.6 mm and channelling angle of ~170 μrad . In order to more accurately simulate the beam tests of the shadowing concept in the SPS, the features of the installed crystal are included by modifying the 2D PDF implemented in *pycolimate* and its thickness. In Fig. 2, the simulated trace space presentation is shown at the crystal and ES. As expected, when the crystal is aligned and orientated with the separatrix such that it channels particles arriving at a horizontal position shadowing the downstream ES, a local density reduction at the wires of the ES can be observed. When the crystal is aligned in volume reflection (VR) a density depleted region is also formed, with particles being kicked back into the machine to circulate another three turns, before being extracted

as part of the tail at large amplitude on the extracted beam. The loss reduction factor for the local shadowing case is shown fully parameterised in Fig. 3, as a function of both crystal transverse position and angle. The area marked with a red circle represents the global minimum.

The maximum loss reduction when the crystal is shadowing and channelling is close to a factor of 2, at a reduction of 44 % with respect to the losses recorded with the crystal in a misaligned, amorphous regime. When shadowing and aligned in VR the crystal provides a loss reduction of approximately 20 %. It is interesting to note the regions of elevated loss levels at the ES when the crystal is misaligned and a beamlet of particles is either channelled or volume reflected directly onto the wire-array composing the septum blade.

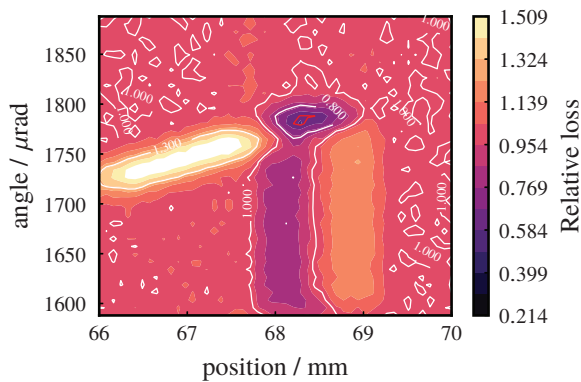


Figure 3: Loss map of the local crystal shadowing system in LSS2: crystal 0.8 mm thick, with 172 mm deflection in channelling. The red contour represents loss reduction of 44 %.

COMPARISON WITH DATA

During the beam tests detailed in [2], multiple angular scans and position scans were performed. As expected from Fig. 3, the minimum of losses in crystal position-angle space is very localised, hence very fine scans were needed to fully characterise the loss reduction profiles and reach the global minimum. In Fig. 4, an angular scan performed with the crystal placed in the optimum position for shadowing is shown in black (LHC-type BLM) and red (SPS-type BLM). In blue, the results from simulations is compared with data showing very good agreement. In Fig. 5, the comparison between simulated (black) and measured (red) position scan in VR is shown. Also in this case, the agreement is shown, although a part of the measured curve could not be properly reproduced with simulations. The reason is to be found in the uncertainty of the crystal angle for each measured position, hence it is difficult to conclude on the error on the measured data.

The effective thickness of the ES can be estimated from a comparison between measurements and simulations. The increase in losses shown in the VR position scan (Fig. 5) is essentially a linear profile of the ES with the well-defined beamlet created by crystal. In fact, the width of the elevated

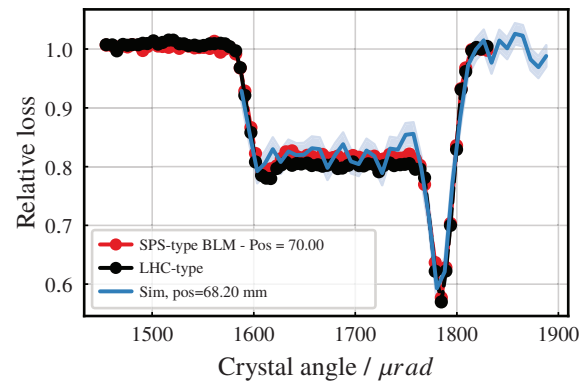


Figure 4: Relative beam loss measured on the BLMs next to the ES during an angular scan of the crystal with it positioned to shadow.

loss peak caused by particles deflected by VR onto the ES is nothing else other than the ES effective width. The thickness estimated in this way is 500 μm, which is in line with what has been obtained from the analysis, combined with simulations, of the diffuser data [8].

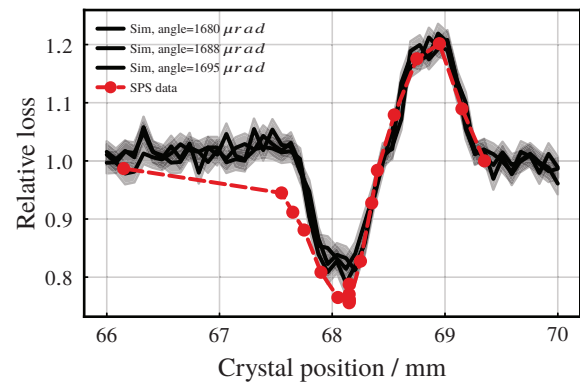


Figure 5: Relative beam loss measured on the BLMs next to the ES as a function of the crystal position when aligned to the beam in volume reflection.

CONCLUSIONS

An extensive simulation campaign of the SPS prototype local crystal shadowing system was presented and compared to empirical data with beam. The simulation tool was used to fully characterise the system by mapping the loss reduction as a function of the available 2D parameter space – crystal alignment in both angle and position. This was possible through a significant improvement in the speed of the simulations using a technique to sectorise the SPS, extract arbitrary order maps from PTC-MAD-X and track in an external, customised tracking routine. The accuracy of the method was shown to be sufficient and the agreement between measurements and simulations achieved led to the estimation of the ZS effective width at 500 μm, which is in line with estimation from the data analysis of the prototype wire-array diffuser.

REFERENCES

- [1] F.M. Velotti, Ph.D. Thesis, Higher brightness beams from the SPS for the HL-LHC era, Ecole Polytechnique de Lausanne, CERN-THESIS-2017-041, 2017.
- [2] F. M. Velotti *et al.*, “Demonstration of Loss Reduction Using a Thin Bent Crystal to Shadow an Electrostatic Septum During Resonant Slow Extraction”, presented at the IPAC’19, Melbourne, Australia, May 2019, paper THXXPLM2, this conference.
- [3] F.M. Velotti *et al.*, Septum shadowing by means of a bent crystal to reduce resonant slow extraction beam loss, submitted to Phys. Rev. Accel. Beams.
- [4] R.Rossi *et al.*, Measurements of coherent interactions of 400 GeV protons in silicon bent crystals, *Nucl. Instrum. Meth. B*, vol. 355, pp. 369 - 373, July 2015.
- [5] Methodical Accelerator Design <https://madx.web.cern.ch>
- [6] V. Kain *et al.*, Resonant slow extraction with constant optics for improved separatrix control at the extraction septum, submitted to Phys. Rev. Accel. Beams.
- [7] P.K. Skowronski *et al.*, Advances in MAD-X using PTC, CERN-LHC-PROJECT-Report-1016, <https://cds.cern.ch/record/1056684>
- [8] B. Goddard *et al.*, Reduction of 400 GeV Slow Extraction Beam Loss with a Wire Diffuser at the CERN SPS, submitted to Phys. Rev. Accel. Beams.
- [9] M.A. Fraser *et al.*, Functional Specification for a Thin Bent Crystal Located in LSS2 for the Shadowing Tests of the ZS wires in 2018, EDMS no. 1783433, CERN, Geneva, Switzerland, 2018.